

The *Arabidopsis* LDL1/2-HDA6 histone modification complex is functionally associated with CCA1/LHY in regulation of circadian clock genes

Fu-Yu Hung^{1,2}, Fang-Fang Chen¹, Chenlong Li^{2,3,4}, Chen Chen^{2,3}, You-Cheng Lai¹, Jian-Hao Chen¹, Yuhai Cui^{2,3,*} and Keqiang Wu^{1,*}

¹Institute of Plant Biology, National Taiwan University, Taipei 10617, Taiwan, ²Agriculture and Agri-Food Canada, London Research and Development Centre, London, Ontario N5V 4T3, Canada, ³Department of Biology, Western University, London, Ontario N6A 3K7, Canada and ⁴State Key Laboratory of Biocontrol and Guangdong Key Laboratory of Plant Resource, School of Life Sciences, Sun Yat-sen University, Guangzhou 510275, China

Received April 24, 2018; Revised August 03, 2018; Editorial Decision August 07, 2018; Accepted August 07, 2018

ABSTRACT

In *Arabidopsis*, the circadian clock central oscillator genes are important cellular components to generate and maintain circadian rhythms. There is a negative feedback loop between the morning expressed CCA1 (CIRCADIAN CLOCK ASSOCIATED 1)/LHY (LATE ELONGATED HYPOCOTYL) and evening expressed TOC1 (TIMING OF CAB EXPRESSION 1). CCA1 and LHY negatively regulate the expression of TOC1, while TOC1 also binds to the promoters of CCA1 and LHY to repress their expression. Recent studies indicate that histone modifications play an important role in the regulation of the central oscillators. However, the regulatory relationship between histone modifications and the circadian clock genes remains largely unclear. In this study, we found that the Lysine-Specific Demethylase 1 (LSD1)-like histone demethylases, LDL1 and LDL2, can interact with CCA1/LHY to repress the expression of TOC1. CHIP-Seq analysis indicated that LDL1 targets a subset of genes involved in the circadian rhythm regulated by CCA1. Furthermore, LDL1 and LDL2 interact with the histone deacetylase HDA6 and co-regulate TOC1 by histone demethylation and deacetylation. These results provide new insight into the molecular mechanism of how the circadian clock central oscillator genes are regulated through histone modifications.

INTRODUCTION

Histone modifications including methylation, acetylation, phosphorylation, ubiquitination and sumoylation play important roles in the regulation of gene expression. All his-

tone modifications are removable, which may therefore provide a flexible way for gene regulation. Methylation on lysine and arginine residues of histone N-terminal tails can be associated with either transcriptional repression or activation. For example, tri-methylation of histone H3 at lysine 4 (H3K4me3) is an active mark for transcription, whereas dimethylation of histone H3 at lysine 9 (H3K9me2) is a signal for transcriptional silencing (1). Histone methylation levels are determined by histone methyltransferases and demethylases, whereas histone acetylation levels are regulated by the action of histone acetyltransferases (HATs) and histone deacetylases (HDACs or HDAs).

Human Lysine-Specific Demethylase 1 (LSD1) is the first histone demethylase identified to demethylate H3K4me through an FAD-dependent oxidation reaction (2). In *Arabidopsis*, four LSD1 homologs have been identified, namely LSD1-LIKE 1 (LDL1), LDL2, LDL3 and FLOWERING LOCUS D (FLD) (3). In *ldl1*, *ldl1/ldl2* and *fld* mutant plants, H3K4 methylation on target genes is enriched, suggesting the H3K4 demethylase activity of LDL1, LDL2 and FLD (3,4). In addition, both *fld* and *ldl1/ldl2* double mutant plants show late flowering phenotypes (3,5). FLD represses the expression of *FLC* by reducing the H3K4me level of *FLC* chromatin (5,6). Furthermore, LDL1 and LDL2 act redundantly to repress the expression of *FLC* by H3K4 demethylation. On the other hand, *ldl1/ldl2* double mutants also show reduced DNA methylation at the *FWA* locus, which represses the floral transition (3).

In yeast and animal systems, HDACs and LSD1 are the core components of several multi-protein complexes, such as Mi2/NuRD and CoREST (7–9). HDACs and LSD1 function cooperatively to regulate gene expression in human breast cancer cells (10). Although the HDAC complexes can dynamically interact with different transcription factors depending on different environmental condi-

*To whom correspondence should be addressed. Tel: +886 2 33664546; Fax: +886 2 33663738; Email: kewu@ntu.edu.tw
Correspondence may also be addressed to Yuhai Cui. Email: yuhai.cui@agr.gc.ca

tions, the interactions between the core protein components in HDAC complexes are relatively stable (11,12). *Arabidopsis* HDA6 is a RPD3-like class I HDAC involved in transcription repression and regulation of ribosomal RNA (13–17). Furthermore, HDA6 is also involved in flowering, leaf development, senescence and abiotic stress response (6,18–20). Recent studies demonstrated that *Arabidopsis* HDA6 interacts directly with FLD and affects flowering time by regulating histone H3 acetylation and H3K4 trimethylation on *FLC*, *MAF4*, and *MAF5* loci (6).

In *Arabidopsis*, the circadian clock central oscillators rely on multiple interconnected loops that generate robust rhythms. There is a negative feedback loop between the morning expressed *CCA1* (*CIRCADIAN CLOCK ASSOCIATED 1*) and *LHY* (*LATE ELONGATED HYPOCOTYL*) as well as the evening expressed *TOC1/PRR1* (*TIMING OF CAB EXPRESSION 1/PSEUDO RESPONSE REGULATOR 1*). *CCA1* and *LHY* are highly accumulated at dawn, but their expression levels are very low in the evening (21–23). *CCA1* and *LHY* proteins inhibit *TOC1* transcription by binding to the evening element (EE) on the *TOC1* promoter (21–23). In the evening, *TOC1* is highly expressed (23). Recent studies indicate that *TOC1* also functions as a repressor and binds to the promoters of *CCA1* and *LHY* to repress their expression in the evening (24,25).

Treating plants with the HDAC inhibitor Trichostatin A (TSA) leads to higher amplitude and delayed phase of *TOC1* expression, but the effect of TSA is reduced in *toc1* mutant plants (26). In addition, the expression level of *CCA1*, *LHY* and *TOC1* is specifically associated with changes in the level of H3K4me and H3 acetylation in *Arabidopsis* (27,28), suggesting that histone modifications are involved in the regulation of circadian central oscillators. Furthermore, the *Arabidopsis* histone acetyltransferase TAF1 and H3K4 methyltransferase SET DOMAIN GROUP 2/ARABIDOPSIS TRITHORAX RELATED 3 (SDG2/ATXR3) may also contribute directly or indirectly to circadian gene activation (28). In addition, HDA6 functions with PRR9 by interacting with TOPLESS/TOPLESS-RELATED (TPL/TPR) and represses *CCA1* transcription (29). These studies indicate that histone modifications play an important role in the regulation of the central oscillators. However, the regulatory relationship between histone modifications and the circadian clock genes remains elusive.

In this study, we found that *LDL1/2* interact with the circadian clock central oscillators *CCA1/LHY*. Furthermore, *LDL1/2* interacts with HDA6 and co-regulate *TOC1* expression by histone demethylation and deacetylation. *LDL1* targets a subset of genes involved in the circadian rhythm regulated by *CCA1*. These results provide new insight into the molecular mechanism of how the circadian clock central oscillator *TOC1* is repressed through histone modifications.

MATERIALS AND METHODS

Plant materials and growth conditions

Arabidopsis (*Arabidopsis thaliana*) was grown in growth chambers under 12/12 h light/dark conditions at 22°C. In

this study, the wild-type *Arabidopsis* Columbia (Col-0) ecotype was used. The mutants used in this research were previously described, including *ldl1/ldl2* (3), *hda6* (*axe1-5*) (6) and *cca1/lhy* (30). *hda6/ldl1/2* triple mutant plants were generated by crossing *ldl1/ldl2* and *hda6* mutant plants.

Plasmid construction and plant transformation

The full-length coding sequence (CDS) fragments of *LDL1*, *LDL2*, *CCA1* and *LHY* were PCR-amplified and cloned into the *pCR8/GW/TOPO* vector (Invitrogen). *HDA6-pCR8/GW/TOPO* was described in previous research (6). *LDL1* and *HDA6* were recombined into the *pEarlyGate103-GFP* or *PK7WGF2* (31) binary vector (Invitrogen), and *LDL1*, *LDL2*, *CCA1* and *LHY* were sub-cloned into 3xFLAG Gateway multiple recombination vectors (<http://www.psb.ugent/gateway/>). Transgenic plants were generated using the floral dip method (32). To construct *LDL1-promoter::LDL1:GFP* or *HDA6-promoter::HDA6:GFP*, *LDL1* or *HDA6* genomic fragment containing ~2 kb promoter was ligated into the modified *pCAMBIA1300* vector containing *GFP*. *pEarlyGate103-LDL1:GFP*, *PK7WGF2-HDA6:GFP*, *LDL1pro::LDL1:GFP* and *HDA6pro::HDA6:GFP* were transformed into *ldl1* and *hda6* by the floral dip method (32).

Bimolecular fluorescence complementation assays

To generate the constructs for BiFC assays, full-length cDNA fragments of *LDL1*, *LDL2*, *CCA1*, *LHY*, *HDA9*, *HDA18*, *GLABRA1* (*GL1/MYB0*) and *MYB23* were PCR-amplified and cloned into the *pCR8/GW/TOPO* vector (Invitrogen), and then recombined into the YN vector *pEarleyGate201-YN* and the YC vector *pEarleyGate202-YC* (33). *HDA6-YN*, *HDA6-YC* and *FLD-YN* were described in previous research (6). Constructed vectors were transiently transformed into *Arabidopsis* protoplasts or tobacco (*Nicotiana benthamiana*) leaves. Transfected protoplasts and leaves were then examined by using a TCS SP5 confocal spectral microscope imaging system (Leica, <https://www.leica.com/>).

Yeast two-hybrid and co-immunoprecipitation assays

Yeast two-hybrid assays were performed according to the instruction for the Matchmaker GAL4-based two-hybrid system 3 (Clontech). Full length or truncated *LDL1*, *LDL2*, *HDA6*, *CCA1* and *LHY* cDNA fragments were sub-cloned into *pGADT7* and *pGBKT7* vectors. All constructs were transformed into the yeast strain AH109 by the lithium acetate method, and yeast cells were grown on a minimal medium/-Leu-Trp according to the manufacturer's instructions (Clontech). Transformed colonies were plated onto a minimal medium/-Leu-Trp-His (3DO) with 0.25 mM 3-amino-1,2,4-triazole(3AT) or media containing X- α -gal for the α -galactosidase activity assay.

Co-immunoprecipitation assays were performed as previously described (6). Anti-GFP (Santa Cruz Biotechnologies, catalog no. SC-9996; 1:3000 dilution), anti-FLAG (SIGMA catalog no. M2; 1:3000 dilution) and anti-CCA1

(Agrisera, catalog no. AS13 2659; 1:500 dilution) antibodies were used as primary antibodies for Western blot, the resulting signals were detected by using a Pierce ECL Western blotting kit (Pierce, <https://www.lifetechnologies.com/>).

Quantitative reverse transcriptase PCR analysis

Total RNA was isolated using TRIZOL reagent (Invitrogen, 15596026) according to the manufacturer's instructions. Two micrograms of DNase (Promega, RQ1 #M6101) treated total RNA were used to synthesize cDNA (Promega, #1012891). RT-qPCR (Real-Time quantitative PCR) was performed using iQ SYBR Green Supermix solution (Bio-Rad, #170-8880). The CFX96 Real-Time PCR Detection System (Bio-Rad Laboratories, Inc.) was used with the following cycling conditions: 95°C for 10 min, followed by 45 cycles of 95°C for 15 s, 60°C for 30 s, and then fluorescent detection. This was immediately followed by a melting curve (65–95°C, incrementing 0.5°C for 5 s, and plate reading). The melting curve analysis confirmed the absence of non-specific products. Each sample was quantified at least in triplicate, and normalized by calculating delta Cq (quantification cycle) to the expression of the internal control *Ubiquitin10* (*UBQ10*). The Cq and relative expression level are calculated by the Biorad CFX Manager 3.1 based on the MIQE guidelines (34). Standard deviations represent at least three technical and two biological replicates. The variance in average data is represented by SEM (standard error of the mean). The SD (standard deviation), SEM determination and *P*-value were calculated using Student's paired *t*-test. The gene specific primers used for qRT-PCR are listed in Supplementary Table S1.

Protoplast transient assays

The native promoter driven *TOC1pro::LUC* plasmid constructs were previously described (30). Effector constructs including *35Spro::TOC1*, *35Spro::CCA1*, *35Spro::LDL1*, *35Spro::HDA6* or *35Spro::GFP* were co-transformed into protoplasts with *TOC1pro::LUC* for transcriptional activity assays, and the plant samples were collected after 12 h at ZT12. The reporter luciferase activities were standardized by activities of co-expressed Renilla luciferase, and relative reporter activities were calculated. Experiments were repeated at least three times for each reporter-effector combination. Signals of Firefly and Renilla luciferase were assayed with the dual luciferase assay reagents (Promega).

Chromatin immunoprecipitation assays

ChIP assays were performed as previously described (6). Chromatin extracts were prepared from seedlings treated with 1% formaldehyde. The chromatin was sheared to the mean length of 500 bp by sonication, proteins and DNA fragments were then immunoprecipitated using antibodies against acetylated histone H3K9K14 (Millipore, catalog no. 06-599), di-methylated histone H3K4 (Diagenode, catalog no. C15410035) or GFP (Abcam, catalog no. ab290). The DNA cross-linked to immunoprecipitated proteins were reversed, and then analyzed by real-time PCR using specific

primers (Supplementary Table S1). Percent input was calculated as follows: $2^{(Cq(IN)-Cq(IP))} \times 100$. Cq is the quantification cycle as calculated by the Biorad CFX Manager 3.1 based on the MIQE guidelines (34). Standard deviations represent at least three technical and two biological replicates. The variance in average data is represented by SEM (standard error of the mean). The SD (standard deviation), SEM determination and *P*-value were calculated using Student's paired *t*-test. The gene specific primers used for real-time PCR are listed in Supplementary Table S1.

ChIP-seq and data analyses

ChIP-seq assays were performed based on previous research (35,36). 10 ng of DNA from at least five ChIPs was pooled to ensure that there are enough starting DNA for library construction. Two biological replicates were prepared and sequenced for each ChIP-seq experiment. The ChIP DNA was first tested by qRT-PCR and then used to prepare ChIP-seq libraries. End repair, adaptor ligation, and amplification were carried out using the Illumina Genomic DNA Sample Prep kit according to the manufacturer's protocol. An Illumina HiSeq 2500 instrument was used for high-throughput sequencing of the ChIP-seq libraries. The raw sequence data were processed using the Illumina sequence data analysis pipeline GAPIipeline 1.3.2. Bowtie (37) was then employed to map the reads to the *Arabidopsis* genome (TAIR10) (38). Only perfectly and uniquely mapped reads were retained for further analysis. To determine the correlation between biological repeats, Pearson correlation was computed using R statistical software on normalized signal intensity for ChIP binding peaks. The alignments were first converted to Wiggle (WIG) files using MACS (39). The data were then imported into the Integrated Genome Viewer (IGV) (40) for visualization. The program SICER (41) was used to identify ChIP-enriched domains (peaks). A peak summit that was positioned within 3 kb upstream or 3 kb downstream of a TSS was assigned to the corresponding gene. If multiple genes could be assigned to a peak, the one with the closest TSS was selected. If no TSS was found in this window, the peak was left unassigned. The overlap venn diagrams were completed by Venny 2.1 (<http://bioinfogp.cnb.csic.es/tools/venny/index.html>). To identify DNA motifs enriched at LDL1-associated sites, 400-bp sequences encompassing each peak summit (200 bp upstream and 200 bp downstream) were extracted and searched for enriched DNA motifs using MEME-ChIP (42). Searches were performed using default parameters. The binding correlation analysis was completed by Expasy ChIP-Seq tools (http://ccg.vital-it.ch/chipseq/chip_cor.php). The LDL1 ChIP-seq data has been deposited to NCBI-Gene Expression Omnibus (GEO) database (GSE118025). ChIP-Seq files from other research groups, GSE67903 (43), GSE70533 (44) and GSE52175 (un-published ChIP-seq data from Nigel P. D.) were downloaded from the NCBI-GEO database.

RESULTS

LDL1 and LDL2 directly interact with CCA1 and LHY

Previous studies indicate that H3K4 methyltransferase activity might be involved in the regulation of circadian cen-

tral oscillators (28). We analyzed whether the *Arabidopsis* H3K4 demethylases LDL1 and LDL2 can interact with CCA1 and LHY. Both LDL1 and LDL2 interacted directly with CCA1 and LHY in Bimolecular Fluorescence Complementation (BiFC) assays by using *Arabidopsis* protoplasts (Figure 1B). Strong YFP signals were observed in the nucleus of the transformed cells. The interactions were further confirmed by yeast two-hybrid (Y2H) assays (Figure 1C, Supplementary Figures S1A and B), Co-immunoprecipitation (Co-IP) assays (Figure 1D, Supplementary Figure S1C) and BiFC assays in *Agrobacterium*-infiltrated tobacco leaves (Supplementary Figures S1D, S2). The interaction between LDL1 and CCA1 at different timing was analyzed by Co-IP assays using *LDL1pro::LDL1::GFP* transgenic *Arabidopsis* plants grown under 12/12 light/dark conditions. Since *CCA1* is highly expressed on ZT0, we found that LDL1 interacted with CCA1 on ZT0 but their interaction was abolished on ZT12 (Figure 1D).

CCA1 β is a splice variant of CCA1, which lacks the MYB-DNA binding domain (45). The N-terminal part of CCA1 β contains an important region (~136–316 aa) for its interaction with LHY and for CCA1 dimerization (45,46). To further investigate the interaction domains, various deletion constructs of LDL1 and CCA1 were generated. The interaction was significantly decreased between CCA1 and LDL1 lacking the N-terminal SWIRM domain (47), but the LDL1 SWIRM domain (LDL1SW) can still strongly interact with CCA1 (Figure 1B, Supplementary Figure S3). These results indicated that the SWIRM domain of LDL1 is mainly responsible for the interaction between CCA1 and LDL1. Although full-length LDL1 can interact with both the N-terminal part (CCA1 β N, 84–316 aa) and C-terminal part of CCA1 β (CCA1 β C, 311–608aa), LDL1SW can only interact with CCA1 β N (Figure 1B, Supplementary Figures S3 and S4).

LDL1/2 and HDA6 acts synergistically to repress the *TOC1* expression by histone deacetylation and H3K4 demethylation

Previous research indicates that *Arabidopsis* HDA6 directly interacts with the H3K4 demethylase FLD and they synergistically co-regulate gene expression by histone deacetylation and H3K4 demethylation (6). We found that HDA6 can also interact with LDL1 and LDL2 in the nucleus in BiFC assays (Figure 2A, Supplementary Figure S5A). In contrast, LDL1 can not interact with HDA9 and HDA18 in BiFC assays (Supplementary Figure S5A). The interactions of LDL1 and LDL2 with HDA6 were further confirmed by Co-IP assays (Figure 2B and C). These results indicate that LDL1/2 and HDA6 may function in the same protein complex to co-regulate gene expression. This is consistent with previous studies in yeast, animal and plant systems, indicating that HDACs and LSD1-like demethylases function cooperatively to regulate gene expression (6–10). Moreover, HDA6 can also interact with CCA1 and LHY in BiFC assays (Supplementary Figure S5B). In comparison, HDA6 and LDL1 cannot interact with two other Myb transcription factors, GLABRA1 (GL1/MYB0) and MYB23. In addition, FLD cannot interact with CCA1 and LHY in BiFC assays (Supplementary Figure S5B). These results indicate

that HDA6 and LDL1 interact with CCA1 and LHY specifically.

The expression of *TOC1* is repressed by CCA1/LHY (22). The interaction of CCA1/LHY with LDL1/2 indicates that they may function together to repress the expression of *TOC1*. We generated the *hda6/ldl1/ldl2* (*hda6/ldl1/2*) triple mutant by crossing *hda6* and *ldl1/ldl2* (*ldl1/2*). Quantitative RT-PCR (qRT-PCR) was used to analyze the daily expression of *TOC1* in Columbia (Col-0) wild type (WT), *hda6*, *ldl1/2* and *hda6/ldl1/2*. The mutant plants were grown under 12 h-light/12 h-dark conditions for 14 days. *TOC1* expression was significantly increased in *ldl1/2* and *hda6* compared to WT (Figure 3A). Furthermore, the expression level of *TOC1* was further increased in *hda6/ldl1/2* compared to *hda6* and *ldl1/2* mutants (Figure 3A). However, the expression phase of *TOC1* was not shifted in the mutant plants compared to WT (Figure 3A). These results indicate that LDL1/2 and HDA6 may act synergistically to repress the expression of *TOC1*, although the daily expression phase of *TOC1* under 12 h-light/12 h-dark conditions is not affected.

To further confirm whether LDL1 can repress *TOC1* expression, the *TOC1* promoter driven *TOC1* fused with *LUCIFERASE* (*TOC1pro::TOC1::LUC* or *pTOC1::LUC*) was co-expressed with *35Spro::CCA1*, *35Spro::LDL1* or *35Spro::GFP* in *Arabidopsis* protoplasts. The *LUC* expression was only slightly decreased when co-expressed with *LDL1*, but significantly decreased when co-expressed with *LDL1* and *CCA1* (Figure 3B). A previous study indicated that co-expression of the full-length CCA1 (CCA1 α) with CCA1 β inhibits the regulatory function of CCA1 (45). We found that CCA1 β can interact with LDL1 and LDL2 in BiFC assays (Figure 1B, Supplementary Figure S3). Interestingly, when LDL1 was co-expressed with CCA1 α and CCA1 β , the *TOC1::LUC* expression level was not significantly repressed (Figure 3B). Taken together, these results indicate that CCA1 functions collaboratively with LDL1 to repress *TOC1*, and the gene repression function of CCA1 and LDL1 was abolished when co-expressed with CCA1 β .

To investigate whether CCA1/LHY affect the levels of H3Ac and H3K4me on *TOC1*, we performed ChIP analysis with WT and *cca1/lhy*. The levels of H3K4me and H3Ac on *TOC1* were significantly increased in *cca1/lhy* compared to WT (Supplementary Figure S6). Previous studies also indicated that H3K4me and H3Ac on *TOC1* were decreased in *CCA1* over-expression plants (26,28). We further analyzed whether LDL1, LDL2 and HDA6 are involved in the regulation of the H3K4me and H3Ac levels of *TOC1*. WT, *ldl1/ldl2*, *hda6* and *hda6/ldl1/2* plants grown under 12h-light/12h-dark conditions for 14-days were collected on ZT0 and ZT12 for ChIP-qPCR assays. The levels of H3K4me and H3Ac on the promoter and exon regions of *TOC1* were significantly increased in both *ldl1/ldl2* and *hda6* compared to WT (Figure 3D), indicating that LDL1, LDL2 and HDA6 are indeed involved in *TOC1* regulation by removing H3K4me and H3Ac. Furthermore, the H3K4me and H3Ac levels were higher in the *hda6/ldl1/2* triple mutant compared to *hda6* and *ldl1/2* (Figure 3D). Similar results were also obtained with additional putative target genes of LDL1, LDL2 and HDA6 (Supplementary Figure S7). These data support that LDL1, LDL2 and

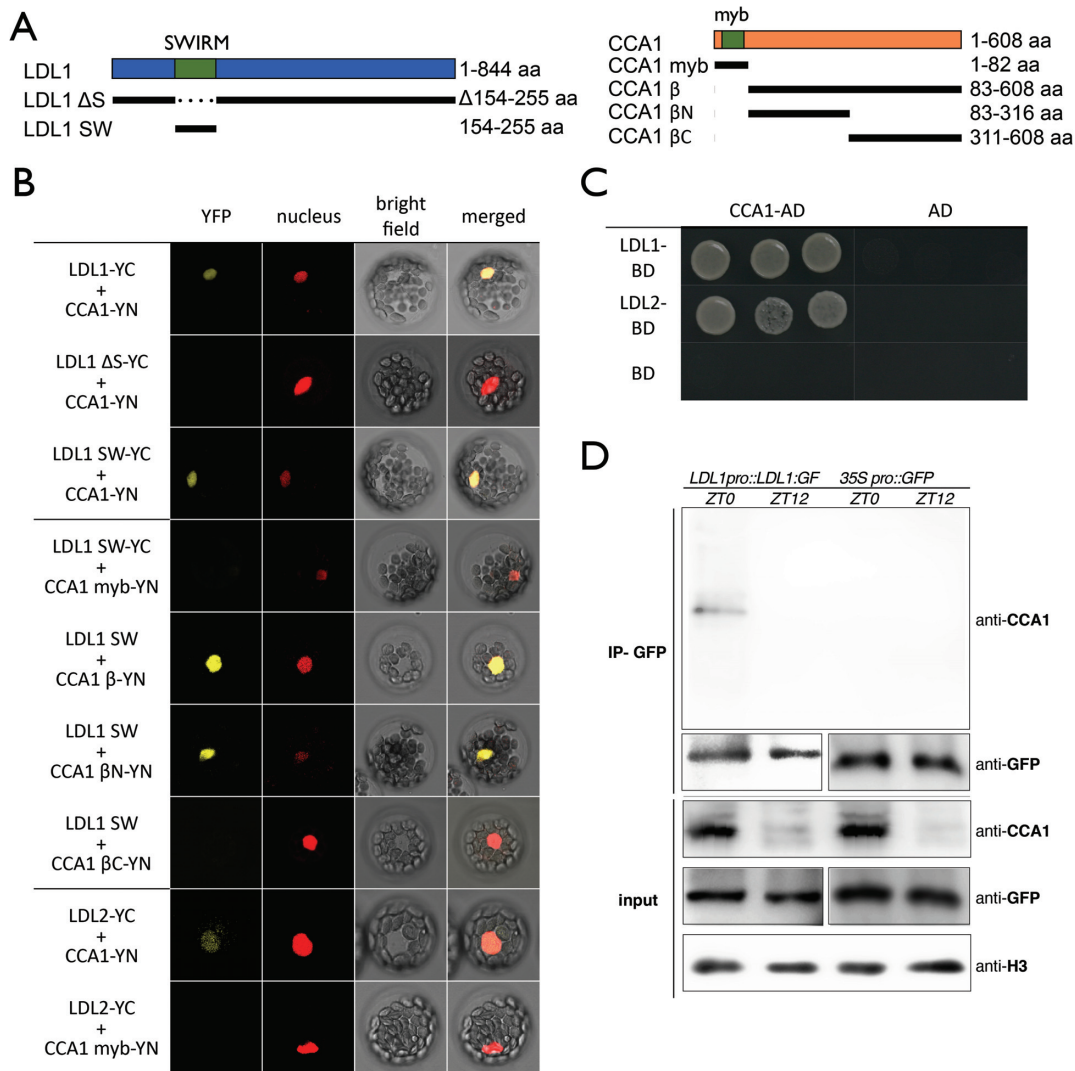


Figure 1. LDL1 and LDL2 interacts with CCA1. (A) Schematic representation of deletions in LDL1 and CCA1 constructs. LDL1 Δ S: deletion of 154–255aa; LDL1SW: 154–255aa; CCA1myb: 1–82aa; CCA1 β : 83–608aa; CCA1 β N: 83–316aa; CCA1 β C: 311–608aa. SWIRM: SWIRM domain of LDL1; myb: myb-domain of CCA1. (B) BiFC assays in *Arabidopsis* protoplasts showing interaction of LDL1/LDL2 with CCA1 in living cells. Different regions of LDL1 and CCA1, and full-length of LDL2 were fused with the N terminus (YN) or C terminus (YC) of YFP and co-delivered into *Arabidopsis* protoplasts. The nucleus was indicated by mCherry carrying a nuclear localization signal. (C) Yeast two hybrid analysis of the interaction of LDL1/LDL2 with CCA1. LDL1-BD/LDL2-BD with CCA1-AD was co-transformed into the yeast strain AH109. The transformants were plated on the SD/-Leu-Trp-His medium. (D) Co-IP of LDL1:GFP with CCA1 in *LDL1pro::LDL1:GFP* transformed *Arabidopsis*. Western blot (WB) was performed with the indicated antibodies.

HDA6 act synergistically to change H3K4me and H3Ac states of their targets.

The LDL1-HDA6 complex targets directly to the *TOC1* promoter

We found that LDL1 interacted with CCA1 on ZT0 but their interaction was abolished on ZT12 (Figure 1D, Supplementary Figure S5C). We further performed ChIP assays to analyze whether LDL1 and HDA6 directly target to *TOC1*. *LDL1:GFP* and *HDA6:GFP* driven by the 35S promoter or their native promoters were transformed into *ldl1* and *hda6* mutants, respectively. Transgenic seedlings were grown under 12/12 light/dark conditions and harvested on ZT0 and ZT12 after 14 days. ChIP assays were performed with the anti-GFP antibody and the binding of LDL1 and

HDA6 to the *TOC1* promoter was analyzed by qPCR. As shown in Figure 4, both LDL1 and HDA6 bound to the *TOC1* promoter. Furthermore, the binding of LDL1 and HDA6 to the *TOC1* promoter was significantly higher on ZT0 than on ZT12 (Figure 4A). The binding of LDL1 and HDA6 to the *TOC1* promoter is correlated with the expression of *TOC1*, since *TOC1* is highly expressed in the evening (22).

To analyze whether the binding of LDL1 and HDA6 to the *TOC1* promoter is dependent on CCA1 and LH1, *LDL1pro::LDL1:GFP* and *HDA6pro::HDA6:GFP* were transformed into the *cca1/lhy* mutant. The binding of LDL1 and HDA6 on the *TOC1* promoter was significantly decreased in *cca1/lhy* on ZT0 (Figure 4B), supporting that the binding of LDL1 and HDA6 to the *TOC1* promoter is dependent on CCA1 and LH1. Although LDL1 and HDA6

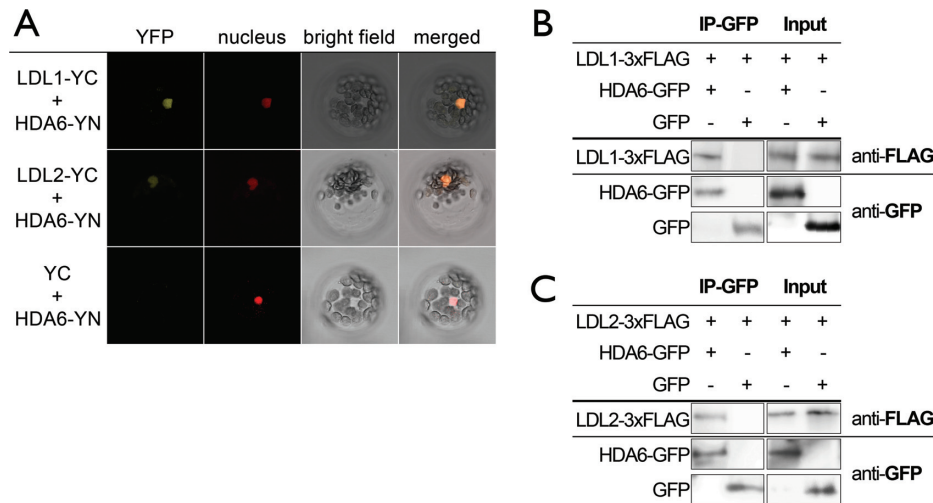


Figure 2. LDL1 and LDL2 interact directly with HDA6. (A) BiFC assays in *Arabidopsis* protoplasts showing interaction of LDL1/LDL2 with HDA6 in living cells. LDL1/LDL2 and HDA6 fused with the N terminus (YN) or C terminus (YC) of YFP were co-delivered into *Arabidopsis* protoplasts. The nucleus was indicated by mCherry carrying a nuclear localization signal. (B, C) Co-IP assays of HDA6:GFP with LDL1-3xFLAG (B) or LDL2-3xFLAG (C). Western blot (WB) was performed with the indicated antibodies.

also bound to the *TOC1* exon regions, this binding was not changed significantly on different time points (Figure 4), indicating that the binding of LDL1 and HDA6 to the *TOC1* exon regions may not depend on CCA1/LHY. Previous studies indicated that H3Ac and H3K4me are involved in both transcription initiation and elongation (48,49). The binding of LDL1 and HDA6 to the *TOC1* exon region implied that LDL1 and HDA6 may also be involved in both transcription initiation and elongation of *TOC1*.

LDL1 and CCA1 co-target genes involved in the circadian rhythm

Since most of the identified *Arabidopsis* circadian clock components display a peak expression at specific times during a day (50,51), we also analyzed the expression patterns of *LDL1*, *LDL2* and *HDA6* in *Arabidopsis* grown under 12/12 light/dark. The expression level of *HDA6* was only slightly increased during dark-period, and the daily expression patterns of *LDL1* and *LDL2* was not changed significantly (Supplementary Figure S8A). In addition, the level of the LDL1 protein did not change significantly on different time points as well (Supplementary Figure S8B). These results indicate that *LDL1*, *LDL2* and *HDA6* are continuously expressed.

We further analyzed the expression of the circadian genes in *ldl1/ldl2* and *hda6/ldl1/2* under ‘free-running’ conditions. Plants grown under 12/12 light/dark for 14 days were transferred to continuous light, and the plant samples were then collected starting from the 2nd day of continuous light. The *TOC1* expression phase was shifted on the 2nd day and 3rd day in *hda6/ldl1/2*. In addition, the expression phase of the circadian marker genes *COLD CIRCADIAN RHYTHM AND RNA BINDING 2* (*CCR2*) and *CHLOROPHYLL A/B-BINDING PROTEIN 2* (*CAB2*) was also shifted in *hda6/ldl1/2* on the 2nd or 3rd days of free-running conditions (Supplementary Figure S8D), indicating that LDL1/2 and HDA6 activities contribute

to the regulation of circadian rhythm. Previous research also indicated that elevated *TOC1* expression causes increased period length (52), which is similar with our results in *hda6/ldl1/2*. The endogenous circadian clock regulates many physiological output processes including hypocotyl growth. We further analyzed hypocotyl lengths of WT, *ldl1/ldl2*, *hda6* and *hda6/ldl1/2*. Similar with *cca1/lhy*, we found that the hypocotyl length of *hda6/ldl1/2* was significantly shorter than WT (Supplementary Figure S9). The circadian phenotypes such as period-shift in gene expression and hypocotyl lengths of *hda6/ldl1/2* indicate that HDA6 and LDL1/2 may act synergistically to regulate circadian central oscillators.

We performed the ChIP sequencing (ChIP-Seq) assays to identify the LDL1-occupied sites in the genome by using the *ldl1* plants expressing *LDL1pro::LDL1:GFP*. Gene Ontology Biological Process (GO-BP) analysis of LDL1-occupied genes indicated that LDL1 regulates a subset of genes involved in circadian rhythms (Figure 5A, Supplementary Table S2). The newly identified LDL1-occupied genes were compared with the previously published CCA1 ChIP-Seq data, GSE67903 (43). Among 863 genes targeted by CCA1, 197 of them were also occupied by LDL1, indicating a high overlap between LDL1 and CCA1 occupied genes ($P = 2.45e-17$) (Figure 5B). Gene Ontology (GO) analysis indicates that the LDL1/CCA1 co-targeted genes contain a higher ratio of the circadian rhythm genes compared to the CCA1-targeted or the LDL1-targeted genes alone (Supplementary Figures S10A and B). Moreover, the binding sites of LDL1 and CCA1 were close to each other (Figure 5C), suggesting that LDL1 and CCA1 tend to bind to the same genomic locations. Similar results were also obtained when compared with another published CCA1 ChIP-Seq data, GSE70533 (44) (Supplementary Figures S10C–E). In addition, we also identified a high binding correlation between the LDL1 genomic binding sites and LHY binding sites when compared the LDL1 ChIP-Seq with the

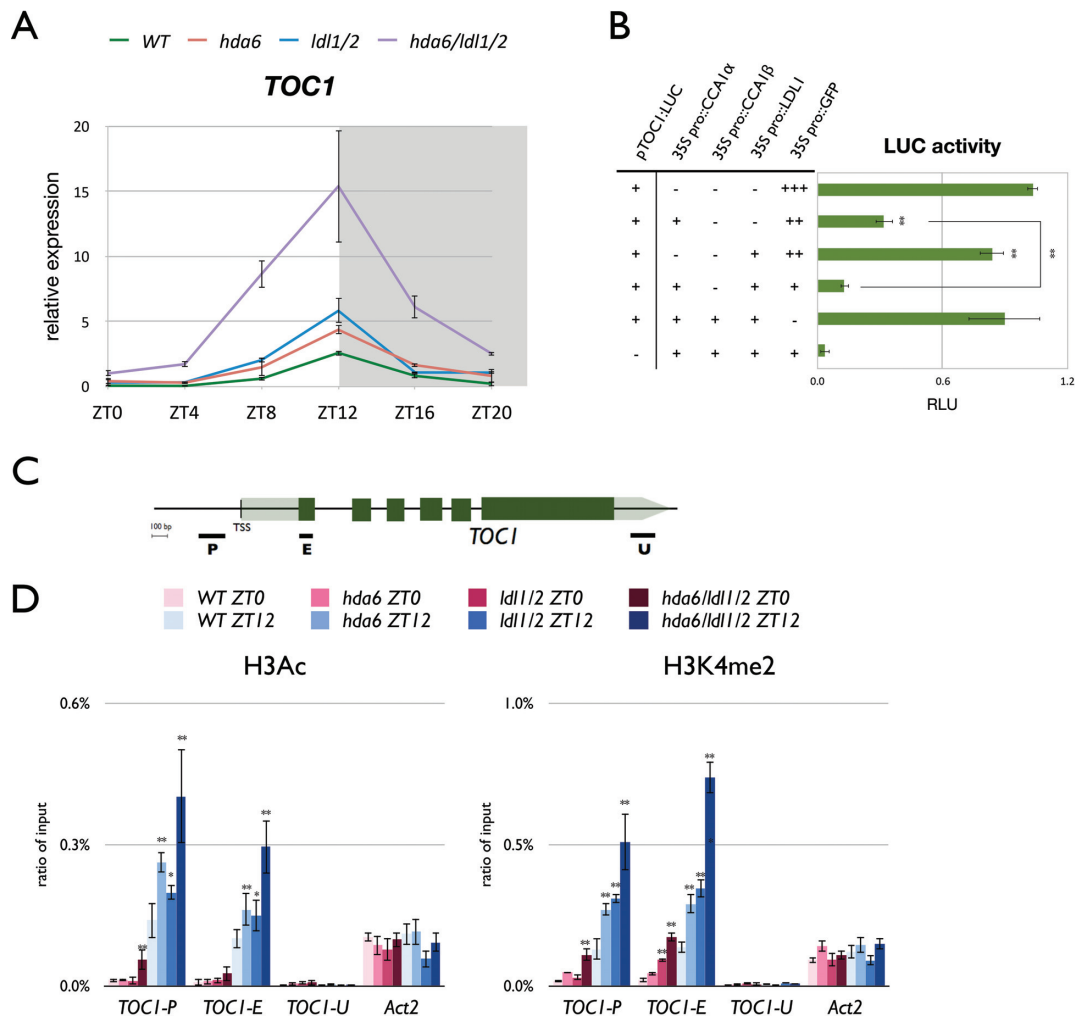


Figure 3. LDL1/LDL2 and HDA6 acts synergistically to repress *TOC1* expression by histone deacetylation and H3K4 demethylation. (A) Gene expression of *TOC1* in WT, *hda6*, *ldl1/2* and *hda6/ldl1/2*. Gene expression was determined by qRT-PCR and normalized to *UBQ10*. Plants were grown under 12/12 light/dark for 14 days. White and grey regions represent light and dark periods, respectively. (B) Transient luciferase assays in *TOC1::LUC* (*pTOC1::LUC*) transformed protoplasts. The CaMV 35S promoter driven *CCA1* (*35S pro::CCA1*) or *LDL1* (*35S pro::LDL1*) effector constructs were introduced into mesophyll protoplasts extracted from WT. Samples were collected on ZT12 after 12h of transformation. Relative Light Units (RLU) represents firefly luciferase normalized by co-expressed *35Spro::Renilla luciferase*. *35Spro::GFP* transformed protoplasts were used as a negative control. (C) Schematic diagram of *TOC1*. P: promoter region, E: coding region, U: 3' UTR. (D) ChIP analysis of H3K9K14ac and H3K4me2 levels of *TOC1*. Plants were grown under 12/12 light/dark for 14 days and plant samples were collected on ZT0 and ZT12. The amounts of DNA after ChIP were quantified by qPCR and values represent the average immunoprecipitation efficiencies (%) against the total input DNA. Data points represent average of three technical replicates. Error bars correspond to standard deviations from three biological replicates. * $P < 0.05$, ** $P < 0.005$ (Student's *t*-test).

LHY ChIP-Seq data, GSE67903 (Supplementary Figure S10F). Previous studies indicate that the *cis*-elements such as the G-box (CACGTG), TCP binding site (TBS, GGC-CCA), Evening Element (EE)-like and (GA/TC)_n repeat were enriched in the CCA1-occupied loci (43,44). Similar *cis*-elements including (GA/TC)_n repeat, G-box, TBS and EE-like motifs were also enriched in LDL1-occupied promoter targets (Figure 5D).

TOC1, *PSEUDORESPONSE REGULATOR 7* (*PRR7*), *PRR9*, *GI*, and *CCR2* as well as the circadian genes *TIME FOR COFFEE* (*TIC*) and *TRF-LIKE 3* (*TRFL3*) were previously identified to be targeted by CCA1 (43,44). These CCA1-occupied genes were also targeted by LDL1. In addition to these genes, we also selected several other genes co-targeted by CCA1/LDL1

for further analysis, including *EUKARYOTIC ELONGATION FACTOR 5A-1* (*ELF5A-1*), *HEAT SHOCK TRANSCRIPTION FACTOR A3* (*HSA3*), *SIGMA FACTOR-BINDING PROTEIN 1* (*SIB1*) and *SERINE CARBOXYPEPTIDASE-LIKE 49* (*SCPL49*) (43,44) (Figure 6A). Genome browser views of the LDL1 ChIP-Seq data indicate that the LDL1 binding peaks were highly correlated with the CCA1 binding regions and close to the G-box, EE or TBS motifs (Figure 6A). The binding of LDL1 to the promoter regions of these CCA1/LDL1 co-targets was also confirmed by ChIP qRT-PCR (Figure 6B). Similar to *TOC1*, we found that the binding of LDL1 to the *CCR2*, *TRFL3*, *GI*, *ELF5A-1*, *HSA3*, *SIB1* and *SCPL49* promoters was significantly higher on ZT0 than ZT12 (Figure 6B). We also analyzed the LDL1 binding

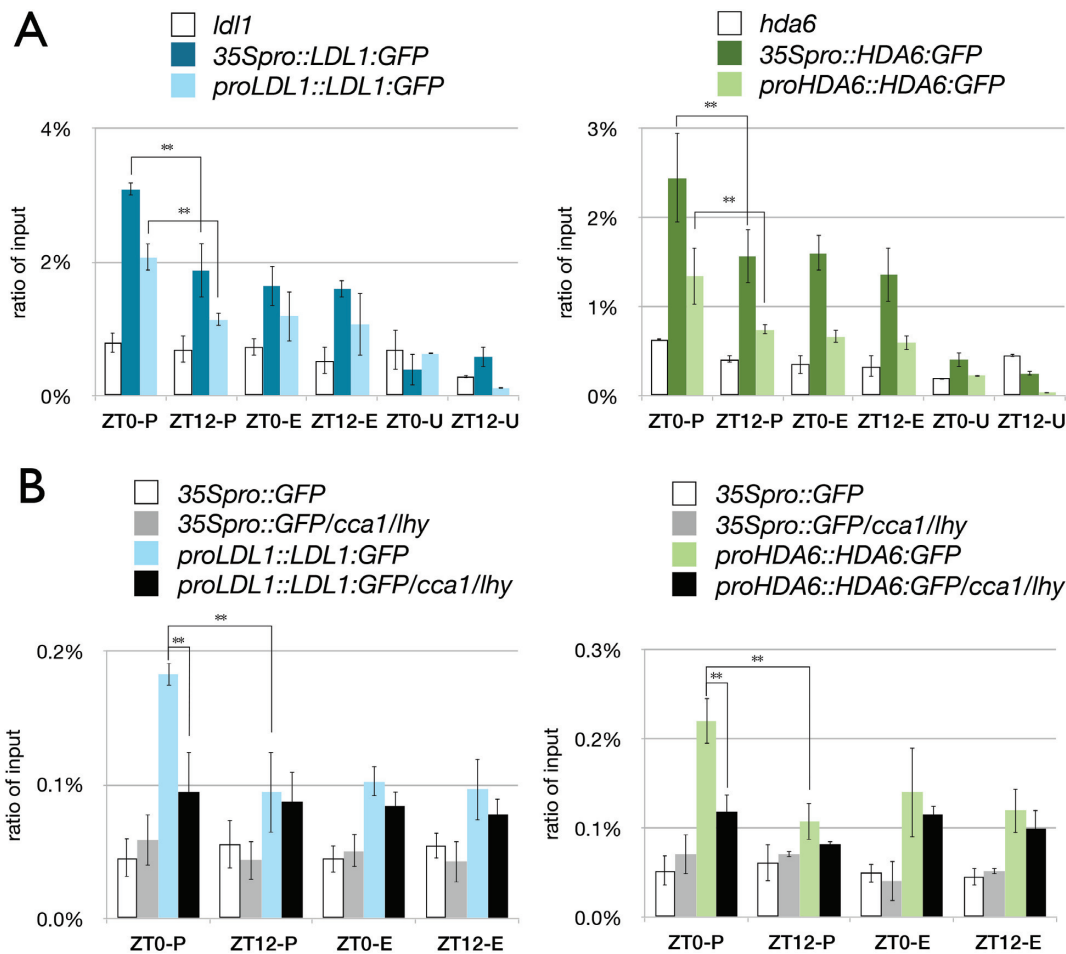


Figure 4. Binding of LDL1 and HDA6 to the *TOC1* promoter *in vivo*. (A, B) LDL1 and HDA6 binding to the *TOC1* promoter. The schematic diagram of *TOC1* is shown in Figure 3. 14 days-old seedlings grown under 12/12 light/dark were harvested on ZT0 or ZT12. ChIP assays were performed with the anti-GFP antibody. The amount of immunoprecipitated DNA was quantified by qRT-PCR. Values represent the average immunoprecipitation efficiencies (%) against the total input DNA. Error bars correspond to standard deviations from three biological replicates. * $P < 0.05$, ** $P < 0.005$ (Student's *t*-test).

to the promoters of the target genes in *cca1/lhy* mutant plants. The binding of LDL1 on all of the above genes was significantly decreased in *cca1/lhy* (Figure 6C), suggesting that the binding of LDL1 to promoter regions of the CCA1/LDL1 co-targets are dependent on CCA1 and LHY.

In addition to *TOC1*, the expression of other CCA1 targets such as *GI* and *CCR2* was also increased in *ldl1/ldl2*, *hda6* and *hda6/ldl1/2* compared to WT (Supplementary Figure S11). The expression of *PRR7* and *PRR9* was decreased in *hda6/ldl1/2* (Supplementary Figure S11). Similarly, the expression of *PRR7* and *PRR9* was also decreased in *cca1/lhy* mutants (53). More recent studies suggested that CCA1 functions as a direct transcription repressor of *PRR7* and *PRR9*, but can act indirectly to activate *PRR7* and *PRR9* in the circadian gene regulatory network (43).

DISCUSSION

There are two types of histone lysine demethylases in eukaryotes, the KDM1/LSD1 and Jumonj C (JmjC) domain-containing demethylases (1,54,55). Four *Arabidopsis* LSD1 homologs including LDL1, LDL2, LDL3 and FLD have

been identified (3). Previous studies indicate that LDL1 and LDL2 act redundantly to repress *FLC* and *FWA* expression, and *ldl1/ldl2* mutants display a significant late flowering phenotype (3). In this study, we found that LDL1/2 are involved in the regulation of the circadian clock genes. Mis-regulation of the circadian oscillators may result in altered flowering phenotypes, but the precise molecular interaction between the clock and flowering is still poorly understood (51). In addition to LSD1-like type histone demethylases, the *Arabidopsis* genome encodes 21 JmjC-domain containing proteins, which are capable of removing the methyl-group on different lysine residues (55,56). JMJ30/JMJ5, a JmjC domain-only group protein, was identified as a H3K27me3 demethylase and can regulate the expression of *CCA1/LHY* (57,58). *Arabidopsis* RELATIVE OF EARLY FLOWERING 6 (REF6) is a H3K27 demethylase with DNA binding activity (35,59). In addition, the KDM5/JARID1 group JmjC domain-containing proteins were also identified as H3K4 demethylases (55,60,61). The roles of these histone demethylase in regulation of the circadian clock have not been investigated. Furthermore, histone H2B mono-ubiquitination (H2bUb)

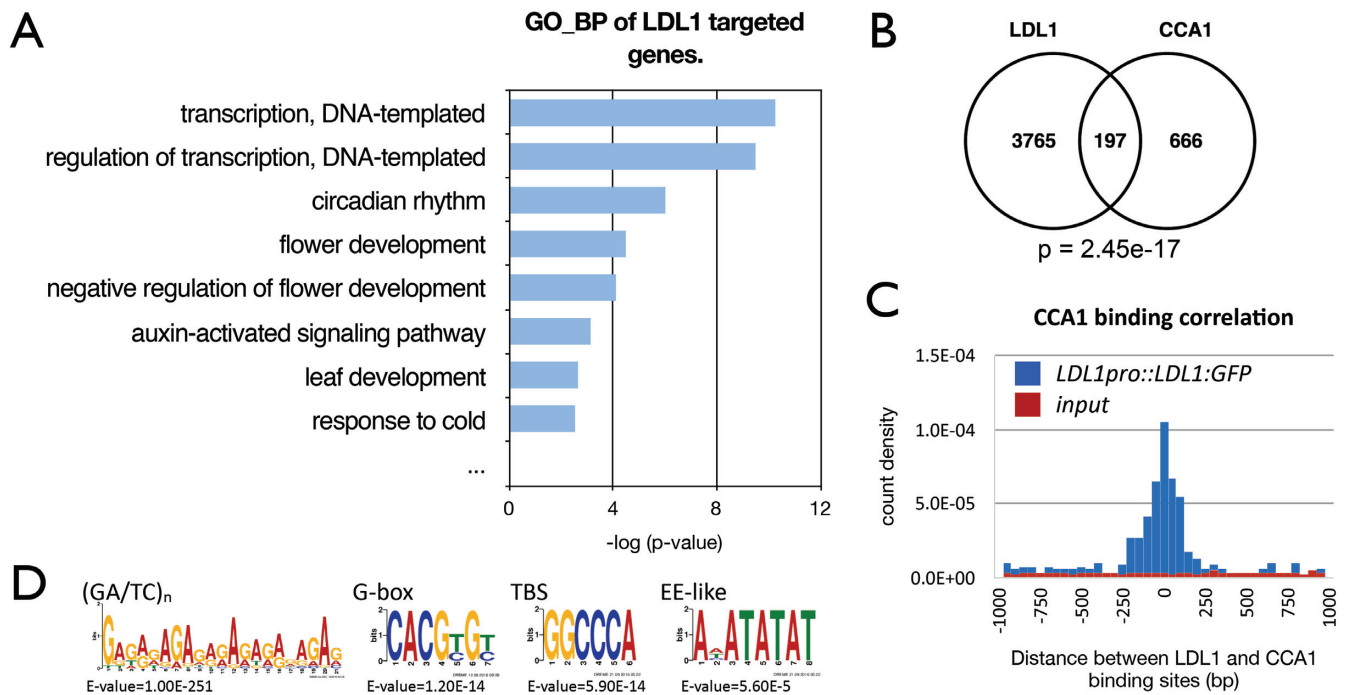


Figure 5. LDL1-occupied sites in the genome identified by ChIP-seq analysis. (A) GO-BP annotation of LDL1-targeted genes. Annotation terms with P -value < 0.005 were listed. (B) Overlap between CCA1 target genes (43) and LDL1 targeted genes. $P = 2.45e-17$ (hypergeometric distribution). (C) Distribution of distances between the total binding sites of LDL1 and CCA1. (D) $(GA/TC)_n$, G-box, TBS and EE-like motifs were significantly enriched in the LDL1-binding sites.

is also associated with the regulation of *CCA1*, *LHY* and *TOC1* (62,63), indicating that H2Bub is involved in regulation of circadian central oscillators. The interaction between LDL1 and the H2B deubiquitinase OTU6/OTLD1 has been reported (64). It remains to be determined whether LDL1 and OTU6/OTLD1 act together to regulate the circadian genes.

In yeast and animal systems, HDACs and LSD1 are identified as the core components of several multi-protein complexes such as Mi2/NuRD and CoREST to regulate gene expression cooperatively (7–10). The *Arabidopsis* LSD1 homolog FLD interacts with HDA6 and regulates flowering (6). In this study, we demonstrate that LDL1/2 can also interact with HDA6 and they act synergistically to regulate gene expression in the circadian clock. Previous studies indicate that HDA6 can be recruited by different transcription factors to regulate gene expression involved in flowering, leaf development, senescence and abiotic stress response (6,12,17–19). In this study, we found that the HDA6-LDL1/2 complex can interact with the Myb-transcription factors CCA1/LHY to regulate *TOC1* expression by removing H3Ac and H3K4me on the *TOC1* locus. Furthermore, more than 300 genes were co-occupied by LDL1 and CCA1 (43,44). Similar cis-elements such as the G-box, TBS, EE and $(GA/TC)_n$ repeat are overrepresented in the binding sites of both CCA1 (43,44) and LDL1, supporting that LDL1 regulates gene expression by interacting with CCA1. *CCA1* and *LHY* are highly expressed in the morning, but their expression levels are very low in the evening (20–22). The interaction between LDL1 and CCA1 was only detectable in the morning in our Co-IP and BiFC analysis.

Furthermore, the binding of LDL1 and HDA6 to the *TOC1* promoter was also decreased in the evening. CCA1/LHY can therefore recruit the histone modification complex containing LDL1/2 and HDA6 to repress the expression of *TOC1* in the morning. However, only about 20% of the putative CCA1-targeted genes were co-targeted by LDL1 in our ChIP-seq experiment, suggesting that maybe not all CCA1 targeted genes are co-regulated by LDL1.

Arabidopsis circadian clock genes generate expression rhythms by multiple interconnected loops and form a complicate feedback regulation network. The central oscillators CCA1, LHY and *TOC1* constitute the central loop (20–23). The central loop is meshed with the morning loop and the evening loop, in which the morning loop contains CCA1/LHY, PRR5, PRR7, and PRR9 (65,66), whereas the evening loop is consist of GI, ZEITLUPE (ZTL), PRR3 and *TOC1* (67–70). We found that although the binding of LDL1 and HDA6 to the *TOC1* promoter region was decreased in the *cca1/lhy* mutant plants, their binding was not completely abolished, suggesting that other unknown transcription factors may also recruit the LDL1/2-HDA6 complex to *TOC1*. In addition to CCA1/LHY, the Evening Complex (EC) comprising of EARLY FLOWERING3 (ELF3), EARLY FLOWERING4 (ELF4) and the small putative Myb transcription factor LUX AR-RHYTHMO (LUX) is also involved in the regulation of *TOC1* (71,72), since *TOC1* expression is increased in *elf3*, *elf4* and *lux* (73–75). It was reported that HDA6 functions with PRR9 by interacting with TOPLESS/TOPLESS-RELATED (TPL/TPR) to repress *CCA1* (29). *TOC1* (also known as PRR1) is one of the PRR-family proteins (76).

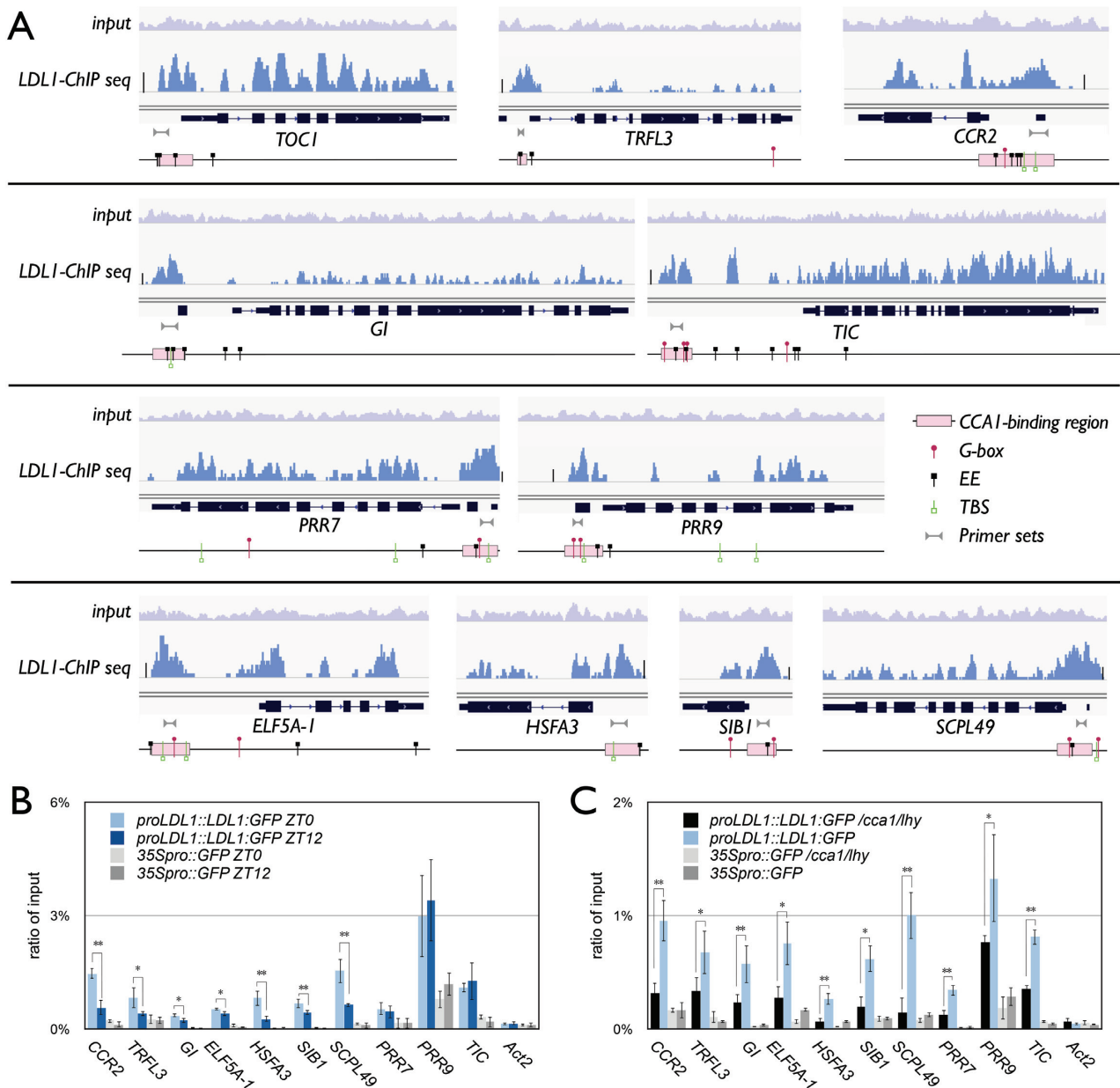


Figure 6. Binding of LDL1 to the CCA1/LDL1 putative co-targets. (A) Integrated Genome View of LDL1-occupied sites on the CCA1-occupied genes. LDL1 binding peaks of LDL1 and CCA1 putative co-targeted genes are shown. Pink bars indicate the CCA1-binding regions from previous published data (43). Bar summits = 50. (B, C) LDL1 binding to the promoters of *CCR2*, *TRFL3*, *GI*, *ELF5A-1*, *HSEF3*, *SIB1*, *SCPL49*, *PRR7*, *PRR9* and *TIC*. 14 days-old seedlings grown under 12/12 light/dark were harvested on ZT0 and ZT12 (B) or ZT0 only (C). ChIP assays were performed with the anti-GFP antibody. The amount of immunoprecipitated DNA was quantified by qRT-PCR. Values represent the average immunoprecipitation efficiencies (%) against the total input DNA. Error bars correspond to standard deviations from three biological replicates. * $P < 0.01$, ** $P < 0.001$ (Student's *t*-test).

The functional correlation of LDL1/2-HDA6 with *TOC1*, *PRRs* and *EC* remains to be further clarified. By using the ChIP-Seq assay, we identified additional circadian genes including the central loop, morning loop and evening loop genes are targeted by LDL1. Since the morning loop and evening loop circadian genes are also involved in the feedback regulation of *CCA1* and *LHY*, it remains to be determined whether this feedback regulation is functional related to LDL1/2 and HDA6.

Recent studies indicated that the circadian clock genes including *TOC1* and *PRRs* are regulated by alternative splic-

ing of RNA transcripts (77–79). While histone acetylation and methylation are important for fine-tuning the accessibility of chromatin, it is believed that pre-mRNA splicing can combine with histone modification events. The association of H3K4me and H3Ac with alternative splicing has been demonstrated in mammalian systems (49,80). In this research, we found that LDL1 and HDA6 can bind to the gene-body of *TOC1*. The ChIP-seq data also showed that LDL1 can bind to the gene-bodies of many circadian genes. These results implied that the LDL1/2-HDA6 complex may be involved in the other regulation processes such as tran-

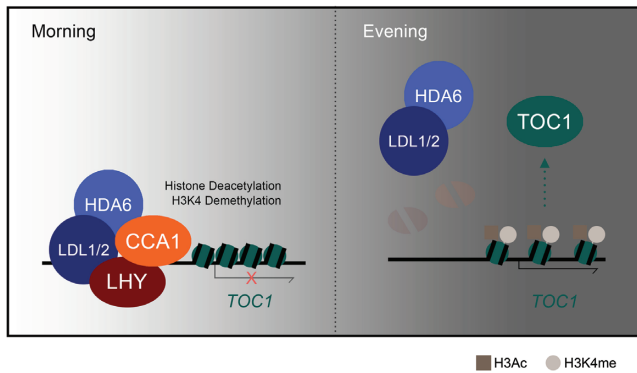


Figure 7. A model for LDL1/2 and HDA6 functions in the regulation of circadian clock central oscillator *TOC1*. The morning accumulated-CCA1/LHY interact with the histone modification complex containing LDL1/2 and HDA6. CCA1/LHY act as transcription repressors and recruit the histone modification complex to their targets loci such as *TOC1*. In the evening, CCA1/LHY are low expressed, and *TOC1* is highly expressed because the LDL1/2-HDA6 complex is released from the *TOC1* promoter.

scription elongation and alternative splicing regulation of the circadian genes.

In summary, we demonstrated how LDL1/2 and HDA6 are involved in the regulation of the circadian central oscillators *TOC1* by histone deacetylation and H3K4 demethylation (Figure 7). The morning accumulated-CCA1/LHY interact with the histone modification complex containing LDL1/2 and HDA6. CCA1/LHY act as transcription repressors and recruit the LDL1/2-HDA6 histone modification complex to their targets locus such as *TOC1*. In the evening, CCA1/LHY are low expressed, and *TOC1* is highly expressed because the LDL1/2-HDA6 complex is released from the *TOC1* promoter.

DATA AVAILABILITY

The LDL1 ChIP-seq data was deposited to NCBI-Gene Expression Omnibus (GEO) database (GSE118025).

SUPPLEMENTARY DATA

Supplementary Data are available at NAR Online.

ACKNOWLEDGEMENTS

We thank Prof. S.-H. Wu. and J.-F. Wu for sharing the *cca1/lhy* double mutant and *TOC1pro::LUC* construct. We also thank Technology Commons, College of Life Science, National Taiwan University for the convenient use of the Bio-Rad real-time PCR system and the confocal spectral microscope imaging systems.

FUNDING

Ministry of Science and Technology of the Republic of China [105-2311-B-002-012-MY3 and 106-2313-B-002-003- to K.W.]; National Taiwan University [106R891501 and 107L893101 to K.W.]; Agriculture and Agri-Food Canada A-base and the National Science and Engineering

Research Council of Canada [RGPIN/04625-2017 to Y.C.]. Funding for open access charge: National Taiwan University.

Conflict of interest statement. None declared.

REFERENCES

- Lan, F., Nottke, A.C. and Shi, Y. (2008) Mechanisms involved in the regulation of histone lysine demethylases. *Curr. Opin. Cell Biol.*, **20**, 316–325.
- Shi, Y., Lan, F., Matson, C., Mulligan, P., Whetstone, J.R., Cole, P.A., Casero, R.A. and Shi, Y. (2004) Histone demethylation mediated by the nuclear amine oxidase homolog LSD1. *Cell*, **119**, 941–953.
- Jiang, D., Yang, W., He, Y. and Amasino, R.M. (2007) *Arabidopsis* relatives of the human lysine-specific Demethylase1 repress the expression of *FWA* and *FLOWERING LOCUS C* and thus promote the floral transition. *Plant Cell*, **19**, 2975–2987.
- Greenberg, M.V.C., Deleris, A., Hale, C.J., Liu, A., Feng, S.H. and Jacobsen, S.E. (2013) Interplay between active chromatin marks and RNA-Directed DNA methylation in *Arabidopsis thaliana*. *PLoS Genet.*, **9**, e1003946.
- He, Y., Michaels, S.D. and Amasino, R.M. (2003) Regulation of flowering time by histone acetylation in *Arabidopsis*. *Science*, **302**, 1751–1754.
- Yu, C.W., Liu, X., Luo, M., Chen, C., Lin, X., Tian, G., Lu, Q., Cui, Y. and Wu, K. (2011) HISTONE DEACETYLASE6 interacts with *FLOWERING LOCUS D* and regulates flowering in *Arabidopsis*. *Plant Physiol.*, **156**, 173–184.
- Khochbin, S., Verdel, A., Lemerrier, C. and Seigneurin-Berny, D. (2001) Functional significance of histone deacetylase diversity. *Curr. Opin. Genet. Dev.*, **11**, 162–166.
- Lee, M.G., Wynder, C., Cooch, N. and Shiekhattar, R. (2005) An essential role for CoREST in nucleosomal histone 3 lysine 4 demethylation. *Nature*, **437**, 432–435.
- Wang, Y., Zhang, H., Chen, Y., Sun, Y., Yang, F., Yu, W., Liang, J., Sun, L., Yang, X., Shi, L. et al. (2009) LSD1 is a subunit of the NuRD complex and targets the metastasis programs in breast cancer. *Cell*, **138**, 660–672.
- Huang, P.H., Chen, C.H., Chou, C.C., Sargeant, A.M., Kulp, S.K., Teng, C.M., Byrd, J.C. and Chen, C.S. (2011) Histone deacetylase inhibitors stimulate histone H3 lysine 4 methylation in part via transcriptional repression of histone H3 lysine 4 demethylases. *Mol. Pharmacol.*, **79**, 197–206.
- Joshi, P., Greco, T.M., Guise, A.J., Luo, Y., Yu, F., Nesvizhskii, A.I. and Cristea, I.M. (2013) The functional interactome landscape of the human histone deacetylase family. *Mol. Syst. Biol.*, **9**, 672.
- Liu, X., Yang, S., Zhao, M., Luo, M., Yu, C.W., Chen, C.Y., Tai, R. and Wu, K. (2014) Transcriptional repression by histone deacetylases in plants. *Mol. Plant*, **7**, 764–772.
- Murfett, J., Wang, X.J., Hagen, G. and Guilfoyle, T.J. (2001) Identification of *Arabidopsis* histone deacetylase HDA6 mutants that affect transgene expression. *Plant Cell*, **13**, 1047–1061.
- Probst, A.V., Fagard, M., Proux, F., Mourrain, P., Boutet, S., Earley, K., Lawrence, R.J., Pikaard, C.S., Murfett, J., Furner, I. et al. (2004) *Arabidopsis* histone deacetylase HDA6 is required for maintenance of transcriptional gene silencing and determines nuclear organization of rDNA repeats. *Plant Cell*, **16**, 1021–1034.
- Earley, K., Lawrence, R.J., Pontes, O., Reuther, R., Enciso, A.J., Silva, M., Neves, N., Gross, M., Viegas, W. and Pikaard, C.S. (2006) Erasure of histone acetylation by *Arabidopsis* HDA6 mediates large-scale gene silencing in nucleolar dominance. *Genes Dev.*, **20**, 1283–1293.
- Liu, X.C., Yu, C.W., Duan, J., Luo, M., Wang, K.C., Tian, G., Cui, Y.H. and Wu, K.Q. (2012) HDA6 directly interacts with DNA methyltransferase MET1 and maintains transposable element silencing in *Arabidopsis*. *Plant Physiol.*, **158**, 119–129.
- Yu, C.W., Tai, R., Wang, S.C., Yang, P., Luo, M., Yang, S., Cheng, K., Wang, W.C., Cheng, Y.S. and Wu, K. (2017) HISTONE DEACETYLASE6 acts in concert with histone methyltransferases SUVH4, SUVH5, and SUVH6 to regulate transposon silencing. *Plant Cell*, **29**, 1970–1983.

18. Wu, K., Zhang, L., Zhou, C., Yu, C.W. and Chaikam, V. (2008) HDA6 is required for jasmonate response, senescence and flowering in *Arabidopsis*. *J. Exp. Bot.*, **59**, 225–234.
19. Chen, L.T., Luo, M., Wang, Y.Y. and Wu, K. (2010) Involvement of *Arabidopsis* histone deacetylase HDA6 in ABA and salt stress response. *J. Exp. Bot.*, **61**, 3345–3353.
20. Luo, M., Yu, C.W., Chen, F.F., Zhao, L., Tian, G., Liu, X., Cui, Y., Yang, J.Y. and Wu, K. (2012) Histone deacetylase HDA6 is functionally associated with AS1 in repression of *KNOX* genes in *Arabidopsis*. *PLoS Genet.*, **8**, e1003114.
21. Schaffer, R., Ramsay, N., Samach, A., Corden, S., Putterill, J., Carre, I.A. and Coupland, G. (1998) The late elongated hypocotyl mutation of *Arabidopsis* disrupts circadian rhythms and the photoperiodic control of flowering. *Cell*, **93**, 1219–1229.
22. Wang, Z.Y. and Tobin, E.M. (1998) Constitutive expression of the *CIRCADIAN CLOCK ASSOCIATED 1 (CCA1)* gene disrupts circadian rhythms and suppresses its own expression. *Cell*, **93**, 1207–1217.
23. Alabadi, D., Oyama, T., Yanovsky, M.J., Harmon, F.G., Mas, P. and Kay, S.A. (2001) Reciprocal regulation between TOC1 and LHY/CCA1 within the *Arabidopsis* circadian clock. *Science*, **293**, 880–883.
24. Gendron, J.M., Pruneda-Paz, J.L., Doherty, C.J., Gross, A.M., Kang, S.E. and Kay, S.A. (2012) *Arabidopsis* circadian clock protein, TOC1, is a DNA-binding transcription factor. *Proc. Natl. Acad. Sci. U.S.A.*, **109**, 3167–3172.
25. Huang, W., Perez-Garcia, P., Pokhilko, A., Millar, A.J., Antoshechkin, I., Riechmann, J.L. and Mas, P. (2012) Mapping the core of the *Arabidopsis* circadian clock defines the network structure of the oscillator. *Science*, **336**, 75–79.
26. Perales, M. and Mas, P. (2007) A functional link between rhythmic changes in chromatin structure and the *Arabidopsis* biological clock. *Plant Cell*, **19**, 2111–2123.
27. Malapeira, J., Khaitova, L.C. and Mas, P. (2012) Ordered changes in histone modifications at the core of the *Arabidopsis* circadian clock. *Proc. Natl. Acad. Sci. U.S.A.*, **109**, 21540–21545.
28. Hemmes, H., Henriques, R., Jang, I.C., Kim, S. and Chua, N.H. (2012) Circadian clock regulates dynamic chromatin modifications associated with *Arabidopsis* CCA1/LHY and TOC1 transcriptional rhythms. *Plant Cell Physiol.*, **53**, 2016–2029.
29. Wang, L., Kim, J. and Somers, D.E. (2013) Transcriptional corepressor TOPLESS complexes with pseudoresponse regulator proteins and histone deacetylases to regulate circadian transcription. *Proc. Natl. Acad. Sci. U.S.A.*, **110**, 761–766.
30. Wang, Y., Wu, J.F., Nakamichi, N., Sakakibara, H., Nam, H.G. and Wu, S.H. (2011) LIGHT-REGULATED WD1 and PSEUDO-RESPONSE REGULATOR9 form a positive feedback regulatory loop in the *Arabidopsis* circadian clock. *Plant Cell*, **23**, 486–498.
31. Karimi, M., Inze, D. and Depicker, A. (2002) GATEWAY vectors for *Agrobacterium*-mediated plant transformation. *Trends Plant Sci.*, **7**, 193–195.
32. Clough, S.J. and Bent, A.F. (1998) Floral dip: a simplified method for *Agrobacterium*-mediated transformation of *Arabidopsis thaliana*. *Plant J.*, **16**, 735–743.
33. Lu, Q., Tang, X., Tian, G., Wang, F., Liu, K., Nguyen, V., Kohalmi, S.E., Keller, W.A., Tsang, E.W., Harada, J.J. et al. (2010) *Arabidopsis* homolog of the yeast *TREX-2* mRNA export complex: components and anchoring nucleoporin. *Plant J.*, **61**, 259–270.
34. Bustin, S.A., Benes, V., Garson, J.A., Hellems, J., Huggett, J., Kubista, M., Mueller, R., Nolan, T., Pfaffl, M.W., Shipley, G.L. et al. (2009) The MIQE guidelines: minimum information for publication of quantitative real-time PCR experiments. *Clin. Chem.*, **55**, 611–622.
35. Li, C.L., Gu, L.F., Gao, L., Chen, C., Wei, C.Q., Qiu, Q., Chien, C.W., Wang, S.K., Jiang, L.H., Ai, L.F. et al. (2016) Concerted genomic targeting of H3K27 demethylase REF6 and chromatin-remodeling ATPase BRM in *Arabidopsis*. *Nat. Genet.*, **48**, 687–693.
36. Li, C.L., Chen, C., Gao, L., Yang, S.G., Nguyen, V., Shi, X.J., Siminovitch, K., Kohalmi, S.E., Huang, S.Z., Wu, K.Q. et al. (2015) The *Arabidopsis* SWI2/SNF2 chromatin remodeler BRAHMA regulates polycomb function during vegetative development and directly activates the flowering repressor Gene *SVP*. *PLoS Genet.*, **11**, e1004944.
37. Langmead, B., Trapnell, C., Pop, M. and Salzberg, S.L. (2009) Ultrafast and memory-efficient alignment of short DNA sequences to the human genome. *Genome Biol.*, **10**, R25.
38. Lamesch, P., Berardini, T.Z., Li, D., Swarbreck, D., Wilks, C., Sasidharan, R., Muller, R., Dreher, K., Alexander, D.L., Garcia-Hernandez, M. et al. (2012) The *Arabidopsis* Information Resource (TAIR): improved gene annotation and new tools. *Nucleic Acids Res.*, **40**, D1202–D1210.
39. Zhang, Y., Liu, T., Meyer, C.A., Eeckhoute, J., Johnson, D.S., Bernstein, B.E., Nussbaum, C., Myers, R.M., Brown, M., Li, W. et al. (2008) Model-based analysis of ChIP-Seq (MACS). *Genome Biol.*, **9**, R137.
40. Robinson, J.T., Thorvaldsdottir, H., Winckler, W., Guttman, M., Lander, E.S., Getz, G. and Mesirov, J.P. (2011) Integrative genomics viewer. *Nat. Biotechnol.*, **29**, 24–26.
41. Zang, C., Schones, D.E., Zeng, C., Cui, K., Zhao, K. and Peng, W. (2009) A clustering approach for identification of enriched domains from histone modification ChIP-Seq data. *Bioinformatics*, **25**, 1952–1958.
42. Machanick, P. and Bailey, T.L. (2011) MEME-ChIP: motif analysis of large DNA datasets. *Bioinformatics*, **27**, 1696–1697.
43. Kamioka, M., Takao, S., Suzuki, T., Taki, K., Higashiyama, T., Kinoshita, T. and Nakamichi, N. (2016) Direct repression of evening genes by CIRCADIANT CLOCK-ASSOCIATED1 in the *Arabidopsis* circadian clock. *Plant Cell*, **28**, 696–711.
44. Nagel, D.H., Doherty, C.J., Pruneda-Paz, J.L., Schmitz, R.J., Ecker, J.R. and Kay, S.A. (2015) Genome-wide identification of CCA1 targets uncovers an expanded clock network in *Arabidopsis*. *Proc. Natl. Acad. Sci. U.S.A.*, **112**, E4802–E4810.
45. Seo, P.J., Park, M.J., Lim, M.H., Kim, S.G., Lee, M., Baldwin, I.T. and Park, C.M. (2012) A self-regulatory circuit of CIRCADIANT CLOCK-ASSOCIATED1 underlies the circadian clock regulation of temperature responses in *Arabidopsis*. *Plant Cell*, **24**, 2427–2442.
46. Lu, S.X., Knowles, S.M., Andronis, C., Ong, M.S. and Tobin, E.M. (2009) CIRCADIANT CLOCK ASSOCIATED1 and LATE ELONGATED HYPOCOTYL function synergistically in the circadian clock of *Arabidopsis*. *Plant Physiol.*, **150**, 834–843.
47. Aravind, L. and Iyer, L.M. (2002) The SWIRM domain: a conserved module found in chromosomal proteins points to novel chromatin-modifying activities. *Genome Biol.*, **3**, RESEARCH0039.
48. Zhao, Y.M., Lu, J., Sun, H., Chen, X., Huang, W.F., Tao, D. and Huang, B.Q. (2005) Histone acetylation regulates both transcription initiation and elongation of *hsp22* gene in *Drosophila*. *Biochem. Biophys. Res. Commun.*, **326**, 811–816.
49. He, R.S. and Kidder, B.L. (2017) H3K4 demethylase KDM5B regulates global dynamics of transcription elongation and alternative splicing in embryonic stem cells. *Nucleic Acids Res.*, **45**, 6427–6441.
50. Hazen, S.P., Naef, F., Quisel, T., Gendron, J.M., Chen, H.M., Ecker, J.R., Borevitz, J.O. and Kay, S.A. (2009) Exploring the transcriptional landscape of plant circadian rhythms using genome tiling arrays. *Genome Biol.*, **10**, R17.
51. Nagel, D.H. and Kay, S.A. (2013) Complexity in the wiring and regulation of plant circadian networks (vol 22, pg R648, 2012). *Curr. Biol.*, **23**, 95–96.
52. Mas, P., Alabadi, D., Yanovsky, M.J., Oyama, T. and Kay, S.A. (2003) Dual role of TOC1 in the control of circadian and photomorphogenic responses in *Arabidopsis*. *Plant Cell*, **15**, 223–236.
53. Farre, E.M., Harmer, S.L., Harmon, F.G., Yanovsky, M.J. and Kay, S.A. (2005) Overlapping and distinct roles of PRR7 and PRR9 in the *Arabidopsis* circadian clock. *Curr. Biol.*, **15**, 47–54.
54. Klose, R.J., Kallin, E.M. and Zhang, Y. (2006) JmjC-domain-containing proteins and histone demethylation. *Nat. Rev. Genet.*, **7**, 715–727.
55. Luo, M., Hung, F.Y., Yang, S.G., Liu, X.C. and Wu, K.Q. (2014) Histone Lysine Demethylases and Their Functions in Plants. *Plant Mol. Biol. Rep.*, **32**, 558–565.
56. Lu, F.L., Li, G.L., Cui, X., Liu, C.Y., Wang, X.J. and Cao, X.F. (2008) Comparative analysis of JmjC domain-containing proteins reveals the potential histone demethylases in *Arabidopsis* and rice. *J. Integr. Plant Biol.*, **50**, 886–896.
57. Jones, M.A., Covington, M.F., DiTacchio, L., Vollmers, C., Panda, S. and Harmer, S.L. (2010) Jumonji domain protein JMJD5 functions in both the plant and human circadian systems. *Proc. Natl. Acad. Sci. U.S.A.*, **107**, 21623–21628.

58. Gan, E.S., Xu, Y.F., Wong, J.Y., Goh, J.G., Sun, B., Wee, W.Y., Huang, J.B. and Ito, T. (2014) Jumonji demethylases moderate precocious flowering at elevated temperature via regulation of *FLC* in *Arabidopsis*. *Nat. Commun.*, **5**, 5098.
59. Lu, F.L., Cui, X., Zhang, S.B., Jenuwein, T. and Cao, X.F. (2011) *FLOWERING LOCUS T* chromatin by functionally redundant histone H3 lysine 27 demethylase. *Nat. Genet.*, **43**, 715–719.
60. Jeong, J.H., Song, H.R., Ko, J.H., Jeong, Y.M., Kwon, Y.E., Seol, J.H., Amasino, R.M., Noh, B. and Noh, Y.S. (2009) Repression of *FLOWERING LOCUS T* chromatin by functionally redundant histone H3 lysine 4 demethylases in *Arabidopsis*. *PLoS One*, **4**, e8033.
61. Yang, H., Mo, H., Fan, D., Cao, Y., Cui, S. and Ma, L. (2012) Overexpression of a histone H3K4 demethylase, JM15, accelerates flowering time in *Arabidopsis*. *Plant Cell Rep.*, **31**, 1297–1308.
62. Himanen, K., Woloszynska, M., Boccardi, T.M., De Groeve, S., Nelissen, H., Bruno, L., Vuylsteke, M. and Van Lijsebettens, M. (2012) Histone H2B monoubiquitination is required to reach maximal transcript levels of circadian clock genes in *Arabidopsis*. *Plant J.*, **72**, 249–260.
63. Bourbousse, C., Ahmed, I., Roudier, F., Zabulon, G., Blondet, E., Balzergue, S., Colot, V., Bowler, C. and Barneche, F. (2012) Histone H2B monoubiquitination facilitates the rapid modulation of gene expression during *Arabidopsis* photomorphogenesis. *PLoS Genet.*, **8**, e1002825.
64. Krichevsky, A., Zaltsman, A., Lacroix, B. and Citovsky, V. (2011) Involvement of KDM1C histone demethylase-OTLD1 otubain-like histone deubiquitinase complexes in plant gene repression. *Proc. Natl. Acad. Sci. U.S.A.*, **108**, 11157–11162.
65. Nakamichi, N., Kiba, T., Henriques, R., Mizuno, T., Chua, N.H. and Sakakibara, H. (2010) PSEUDO-RESPONSE REGULATORS 9, 7, and 5 are transcriptional repressors in the *Arabidopsis* circadian clock. *Plant Cell*, **22**, 594–605.
66. Salome, P.A., Weigel, D. and McClung, C.R. (2010) The role of the *Arabidopsis* morning loop components CCA1, LHY, PRR7, and PRR9 in temperature compensation. *Plant Cell*, **22**, 3650–3661.
67. Kim, W.Y., Geng, R. and Somers, D.E. (2003) Circadian phase-specific degradation of the F-box protein ZTL is mediated by the proteasome. *Proc. Natl. Acad. Sci. U.S.A.*, **100**, 4933–4938.
68. Para, A., Farre, E.M., Imaizumi, T., Pruneda-Paz, J.L., Harmon, F.G. and Kay, S.A. (2007) PRR3 Is a vascular regulator of TOC1 stability in the *Arabidopsis* circadian clock. *Plant Cell*, **19**, 3462–3473.
69. McClung, C.R. and Gutierrez, R.A. (2010) Network news: prime time for systems biology of the plant circadian clock. *Curr. Opin. Genet. Dev.*, **20**, 588–598.
70. Mas, P., Kim, W.Y., Somers, D.E. and Kay, S.A. (2003) Targeted degradation of TOC1 by ZTL modulates circadian function in *Arabidopsis thaliana*. *Nature*, **426**, 567–570.
71. Nusinow, D.A., Helfer, A., Hamilton, E.E., King, J.J., Imaizumi, T., Schultz, T.F., Farre, E.M. and Kay, S.A. (2011) The ELF4-ELF3-LUX complex links the circadian clock to diurnal control of hypocotyl growth. *Nature*, **475**, 398–402.
72. Pokhilko, A., Fernandez, A.P., Edwards, K.D., Southern, M.M., Halliday, K.J. and Millar, A.J. (2012) The clock gene circuit in *Arabidopsis* includes a repressilator with additional feedback loops. *Mol. Syst. Biol.*, **8**, 574.
73. Kolmos, E., Nowak, M., Werner, M., Fischer, K., Schwarz, G., Mathews, S., Schoof, H., Nagy, F., Bujnicki, J.M. and Davis, S.J. (2009) Integrating ELF4 into the circadian system through combined structural and functional studies. *HFSP J.*, **3**, 350–366.
74. Dixon, L.E., Knox, K., Kozma-Bognar, L., Southern, M.M., Pokhilko, A. and Millar, A.J. (2011) Temporal repression of core circadian genes is mediated through EARLY FLOWERING 3 in *Arabidopsis*. *Curr. Biol.*, **21**, 120–125.
75. Hazen, S.P., Schultz, T.F., Pruneda-Paz, J.L., Borevitz, J.O., Ecker, J.R. and Kay, S.A. (2005) *LUX ARRHYTHMO* encodes a Myb domain protein essential for circadian rhythms. *Proc. Natl. Acad. Sci. U.S.A.*, **102**, 10387–10392.
76. Matsushika, A., Makino, S., Kojima, M. and Mizuno, T. (2000) Circadian waves of expression of the *APRR1/TOC1* family of pseudo-response regulators in *Arabidopsis thaliana*: insight into the plant circadian clock. *Plant Cell Physiol.*, **41**, 1002–1012.
77. Jones, M.A., Williams, B.A., McNicol, J., Simpson, C.G., Brown, J.W. and Harmer, S.L. (2012) Mutation of *Arabidopsis* spliceosomal timekeeper locus1 causes circadian clock defects. *Plant Cell*, **24**, 4066–4082.
78. Perez-Santangelo, S., Schlaen, R.G. and Yanovsky, M.J. (2013) Genomic analysis reveals novel connections between alternative splicing and circadian regulatory networks. *Brief. Funct. Genomics*, **12**, 13–24.
79. Perez-Santangelo, S., Mancini, E., Francey, L.J., Schlaen, R.G., Chernomoretz, A., Hogenesch, J.B. and Yanovsky, M.J. (2014) Role for *LSM* genes in the regulation of circadian rhythms. *Proc. Natl. Acad. Sci. U.S.A.*, **111**, 15166–15171.
80. Shindo, Y., Nozaki, T., Saito, R. and Tomita, M. (2013) Computational analysis of associations between alternative splicing and histone modifications. *FEBS Lett.*, **587**, 516–521.